Universiteit Utrecht

Faculteit Bètawetenschappen

Bachelor Thesis
Opleiding Natuur- en Sterrenkunde

Theory and experiments on soliton interactions

Author:
Simon Veldkamp

Supervisor
Prof. Dr. Leo Maas
Imau

June 14, 2017

Abstract

The behaviour of surfacewaves on shallow water is described by nonlinear differential equations. Putting a constraint on these equation, such that they only describe waves moving in a certain direction, one obtains the KdV-equation. This nonlinear partial differential equation has the surprising property that it admits stable solutions. In these solutions dispersive and nonlinear effects balance out, creating what is known as a soliton. For certain initial conditions the KdV-equation can be solved analytically by using the inverse scattering transform. This method shows that, for a certain initial condition, there is a one-to-one correspondence between the solitons that emerge from this condition, and the eigenvalues of the time-independent Schrodinger equation, where the potential is given by this initial condition. Furthermore, it shows that when co-propagating solitons overtake each other they maintain their shape and velocity, but obtain a phase difference. A solution for the system where waves are not constraint to a single direction has not been found yet. However using both numerical and analytic methods it has been shown that for both reflection at a vertical wall and head on collision between solitons, a phaselag occurs. Here experiments on reflection and head-on collisions of solitons are compared to these analytic and numerical results to show that indeed a phaselag occurs at reflection.

Contents

1 Introduction

In 1834 the Scottish engineer John Scott Russel, spotted an interesting phenomenon in a canal. Of which he gave the following account:

"I was observing the motion of a boat which was rapidly drawn along a narrow channel by a pair of horses, when the boat suddenly stopped—not so the mass of water in the channel which it had put in motion; it accumulated round the prow of the vessel in a state of violent agitation, then suddenly leaving it behind, rolled forward with great velocity, assuming the form of a large solitary elevation, a rounded, smooth and well-defined heap of water, which continued its course along the channel apparently without change of form or diminution of speed. I followed it on horseback, and overtook it still rolling on at a rate of some eight or nine miles an hour, preserving its original figure some thirty feet long and a foot to a foot and a half in height. Its height gradually diminished, and after a chase of one or two miles I lost it in the windings of the channel. Such, in the month of August 1834, was my first chance interview with that singular and beautiful phenomenon which I have called the Wave of Translation."

What Russel observed is now known as a soliton; a stable solitary wave, with a few interesting properties. They can travel over long distances without changing much in shape, bigger waves travel faster than smaller waves and when a soliton overtakes another one they emerge unchanged. In 1895 Korteweg and De Vries derived an equation for waves in shallow water, known as the KdV-Equation:

$$u_t - 6uu_x + u_{xxx} = 0. \tag{1}$$

Even though this equation is nonlinear, it can be solved. From this many of the things John Scott Russel discovered about them can be shown analytically. One of the things that follows from this analysis is that when a soliton overtakes a smaller soliton, they indeed retain their shape and speed. However, a small phase-shift occurs; the bigger soliton ends up a bit further than if it hadn't met the smaller soliton, while the smaller soliton lags a bit behind. We could now ask what happens when two solitons interact by a head-on collision. This however is much harder to do analytically. The KdV-equation is designed to describe waves moving from left to right or vice-versa, and can therefore not describe waves moving in opposite directions in the same system. In this thesis I will look at the derivation of the KDV-equation (1), to show why it is unidirectional, and which equation can describe a system with solitons moving in opposite directions. Furthermore, I will describe the analytic solution of the KdV-equation, and do experiments on soliton collisions and reflections at a vertical wall, to see if a phaselag occurs here as well.

2 Derivation KdV-equation

This section is mostly based on Whitham Linear and Nonlinear Waves chapter 13 [1]

Firstly we assume to have an incompressible fluid in a constant gravitational field. Furthermore, we assume that the mass density ρ is constant. Under these conditions our system is described by the following equations:

$$\vec{\nabla} \cdot \vec{u} = 0 \tag{2}$$

$$\frac{D\vec{u}}{Dt} = \frac{\partial \vec{u}}{\partial t} + (\vec{u} \cdot \vec{\nabla})\vec{u} = -\frac{1}{\rho}\vec{\nabla}p - g\hat{j}. \tag{3}$$

If we assume the flow to be irrotational, then we can define a potential φ such that $\vec{u} = \vec{\nabla}\varphi$. We can write equation (3) in terms of φ:

$$\vec{\nabla}\dot{\varphi} + \frac{1}{2}\vec{\nabla}(\vec{\nabla}\varphi)^2 = -\frac{1}{\rho}\vec{\nabla}p - \vec{\nabla}(gy). \tag{4}$$

This can be integrated to obtain Bernoulli's Law

$$\frac{p - p_0}{\rho} = -\varphi_t - \frac{1}{2}(\vec{\nabla}\varphi)^2 - gy. \tag{5}$$

Now we define our water surface as a function of time by:

$$f(x_1, x_2, y, t) = 0. \tag{6}$$

Since the fluid cannot cross this surface line by definition, the velocity of the fluid, normal to the surface, must be equal to the velocity of the surface, normal to itself. The normal velocity of the surface is given by:

$$\frac{-f_t}{\sqrt{(f_{x_1}^2 + f_{x_2}^2 + f_y^2)}}, \tag{7}$$

while the velocity of the fluid, normal to the surface, is equal to:

$$\frac{u_1 f_{x_1} + u_2 f_{x_2} + v f_y}{\sqrt{(f_{x_1}^2 + f_{x_2}^2 + f_y^2)}}. \tag{8}$$

Here we use u_1 and u_2 for the horizontal velocities, and v for the vertical velocity. The condition that equations (7) and (8) are equal implies:

$$\frac{Df}{Dt} = 0. \tag{9}$$

Now we will introduce the function η to describe the surface as a function of x_1 and x_2 such that:

$$f(x_1.x_2, y, t) \equiv \eta(x_1, x_2, t) - y. \tag{10}$$

Together with equation (9) we obtain the following condition:

$$\frac{D\eta}{Dt} = \eta_t + u_1\eta_{x_1} + u_2\eta_{x_2} = v. \tag{11}$$

This gives a condition on the movement of the boundary, directly deduced from the definition of the boundary. A second boundary condition can be deduced from equation (4), i.e. from the fluid mechanics of the system.

At the boundary the pressure can be assumed to be equal to the air pressure p_0, for differences in the air pressure due to the motion of our surface are negligible, assuming that there are no external factors influencing the air pressure. So assuming $p = p_0$ we get the following equations on the boundary(surface):

$$\begin{aligned} \eta_t + \varphi_{x_1}\eta_{x_1} + \varphi_{x_2}\eta_{x_2} &= \varphi_y \\ \varphi_t + \frac{1}{2}(\varphi_{x_1}^2 + \varphi_{x_2}^2 + \varphi_y^2) + g\eta &= 0. \end{aligned} \tag{12}$$

These two equations give a single boundary condition on the surface. The reason we need two equations for the boundary condition, instead of one, is because the boundary itself is not fixed. Another boundary in our system is the bottom, here the same formula can be used, with $y = -h_0(x_1, x_2)$. Assuming the bottom is fixed in time, the boundary condition is given by:

$$\varphi_{x_1}h_{x_1} + \varphi_{x_2}h_{x_2} + \varphi_y = 0. \tag{13}$$

When the bottom is flat $h_0(x_1, x_2)$ is a constant, and the boundary condition simplifies to:

$$\varphi_y = 0. \tag{14}$$

2.1 Linearisation

If we assume the water to be at rest, and add small perturbations, we can investigate how the equations behave up to first-order. The boundary conditions derived in the preceding section then become:

$$\eta_t = \varphi_y, \qquad \varphi_t + g\eta = 0. \tag{15}$$

Decoupling y and η by applying the boundary conditions to $y = 0$ instead of $y = \eta$ gives the following system of equations:

$$\begin{aligned} \varphi_{x_1x_1} + \varphi_{x_2x_2} + \varphi_{yy} &= 0, && -h_0 < y < 0 \\ \varphi_{tt} + g\varphi_y &= 0, && y = 0 \\ \varphi_y + h_{0x_1}\varphi_{x_1} + h_{0x_2}\varphi_{x_2} &= 0, && y = -h_0. \end{aligned} \tag{16}$$

This system can be solved when initial conditions are added. The surface is then given by:

$$\eta(x_1, x_2, t) = -\frac{1}{g}\varphi_t(x_1, x_2, 0, t). \tag{17}$$

We can determine the dispersion relation of the linearised system. Waves will propagate horizontally with amplitude dependent on the depth. The elementary sinusoidal solutions take the form:

$$\eta = Ae^{i\vec{\kappa}\cdot\vec{x}-i\omega t}, \qquad \varphi = Y(y)e^{i\vec{\kappa}\cdot\vec{x}-i\omega t}. \tag{18}$$

When we put this expression for φ into the Laplace equation, it gives the following condition on Y:

$$Y_{yy} - \kappa^2 Y = 0, \tag{19}$$

therefore $Y = Ce^{i|\kappa|y} + De^{-i|\kappa|y}$. Combining this with the condition on the bottom, i.e. $Y_y = 0$ on $y = -h_0$, gives:

$$Y = C\cosh(|\kappa|(h_0 + y)).$$

From equation (17) it follows that:

$$A = \frac{i\omega}{g}Y(0).$$

So we can write Y in terms of the amplitude A of η as:

$$Y = -\frac{igA}{\omega}\frac{\cosh|\kappa|(h_0 + y)}{\cosh|\kappa|h_0}. \tag{20}$$

Combining this with the condition on $y = 0$, (16) gives the dispersion relation:

$$\omega^2 = g|\kappa|\tanh|\kappa|h_0. \tag{21}$$

Thus when $\frac{a}{h_0}$ is small, with a the typical amplitude of the wave, we have the dispersion relation found above. When $|\kappa|h_0$ is very small, this relation is approximated by $\omega^2 = gh_0\kappa^2$, which is the dispersion relation of the normal wave equation: $\eta_{tt} - c_0^2\eta_{xx} = 0$.

We can reach this equation in two ways. The first way is linearising the equations first, then finding the dispersion relation, and then taking the first order term in this relation. The other way starts with stating that $\frac{h_0^2}{l^2}$ is small and then linearising the result by stating: $\frac{a}{h_0}$ is small.

The second approach goes as follows. We have the equations:

$$\vec{\nabla}\cdot\vec{u} = 0 \tag{22}$$

$$\frac{D\vec{u}}{Dt} = \frac{\partial\vec{u}}{\partial t} + (\vec{u}\cdot\vec{\nabla})\vec{u} = -\frac{1}{\rho}\vec{\nabla}p - g\hat{j}. \tag{23}$$

If we assume $\frac{Dv}{Dt} = v_t + uv_x + vv_y = 0$, which means that we assume the vertical speed to be constant, the following relation for the pressure is obtained:

$$-\frac{1}{\rho}\frac{\partial p}{\partial y} - g = 0. \tag{24}$$

Integration w.r.t. y gives:

$$p - p_0 = \rho g(\eta - y). \tag{25}$$

Then equation (23) becomes:

$$u_t + uu_x + vu_y = -g\eta_x. \tag{26}$$

Now the only term that depends on y is vu_y therefore if $u_y = 0$ it stays this way. So assuming this we get:

$$u_t + uu_x + g\eta_x = 0. \tag{27}$$

When we integrate $\vec{\nabla}u = 0$ from $-h_0$ to $y = \eta(x)$ we get:

$$0 = \int_{-h_0}^{\eta(x)} u_x + v_y dy = \frac{d}{dx}\int_{-h_0}^{\eta(x)} u dy + [v]_{-h_0}^{\eta(x)} - [u]_{\eta(x)}\eta_x. \tag{28}$$

Using $v = 0$ on the bottom and equation (11) this becomes:

$$\frac{\partial}{\partial x}(h_0 + \eta) + \eta_t = 0. \tag{29}$$

Writing $h = h_0 + \eta$ we then get two equations:

$$\begin{aligned} u_t + uu_x + g\eta_x &= 0 \\ h_t + (hu)_x &= 0. \end{aligned} \tag{30}$$

Linearising these equations gives us:

$$u_{tt} + g\eta_{xt} = 0 \tag{31}$$

$$\eta_{tx} + h_0 u_{xt} = 0. \tag{32}$$

If we multiply the second equation by g and subtract it from the first one, we find the wave equation for η.

$$\eta_{tt} = gh_0\eta_{xx}. \tag{33}$$

To get these equations we estimated $\frac{Dv}{Dt} = 0$. The error this gives in the pressure can be estimated by $v_t\rho h_0$. Furthermore $\vec{\nabla}u = 0$ implies that v is approximately: $h_0 u_x$, so the error in equation (27) is of order:

$$\frac{-p_x}{\rho u_t} \approx \frac{h_0^2 u_{xxt}}{u_t} \approx \frac{h_0^2}{l^2}.$$

Earlier we found the dispersion relation

$$\omega^2 = g\kappa \tanh \kappa h_0$$

by assuming small amplitudes. Assuming $\frac{h_0^2}{l^2} << 1$ then gives the dispersion relation $\omega^2 = gh_0\kappa^2$, which agrees with equation (33). Schematically this looks like this:

$$\begin{array}{ccc} \vec{\nabla}\cdot\vec{u}, \quad \frac{D\vec{u}}{Dt} = \frac{\partial \vec{u}}{\partial t} + (\vec{u}\cdot\vec{\nabla})\vec{u} = -\frac{1}{\rho}\vec{\nabla}p - g\hat{j} & \xrightarrow{\frac{a}{h_0}<<1} & \omega^2 = g\kappa\tanh\kappa h_0 \\ \downarrow{\scriptstyle \frac{h_0^2}{l^2}<<1} & & \downarrow{\scriptstyle \frac{h_0^2}{l^2}<<1} \\ u_t + uu_x + g\eta_x = 0, \quad h_t + (hu)_x = 0 & \xrightarrow{\frac{a}{h_0}<<1} & \eta_{tt} = gh_0\eta_{xx} \end{array}$$

2.2 Higher order expressions

Now we can use a more formal approach to find equation corresponding to higher order terms in $\frac{h_0^2}{l^2}$ and $\frac{a}{h_0}$. We start out by normalizing the variables to be:

$$x' = lx, \qquad Y' = h_0 Y, \qquad t' = \frac{lt}{c_0}$$
$$\eta' = a\eta, \qquad \varphi' = \frac{gla\varphi}{c_0},$$

here the originial variables are primed. The Laplace equation in our new variables is:

$$\frac{h_0^2}{l^2}\varphi_{xx} + \varphi_{YY} = 0 \tag{34}$$

If we assume φ_x to be approximately independent of Y, then we can introduce a series expansion for φ of the form:

$$\varphi = \sum_0^\infty Y^n f_n(x,t).$$

The Laplace equation then implies: $\frac{h_0^2}{l^2}\frac{\partial^{2m}\varphi}{\partial x^{2m}} = (-1)^m \frac{\partial^{2m}\varphi}{\partial Y^{2m}}$, thus for even powers in the expansion we get:

$$\frac{h_0^2}{l^2}\frac{\partial^{2m} f_0}{\partial x^{2m}} = (-1)^m f_{2m} 2m!,$$

and for odd powers:

$$\frac{h_0^2}{l^2}\frac{\partial^{2m} f_1}{\partial x^{2m}} = (-1)^m f_{2m+1} 2m!.$$

If we use the boundary condition on the bottom, i.e. $\varphi_Y = 0$ on $Y = 0$, we see that $f_1 = 0$, and thus all the odd terms are zero. Writing $\beta = \frac{h_0^2}{l^2}$, and using the relations found above we get the following expression for the expansion of φ:

$$\varphi = \sum_0^\infty (-1)^m \frac{Y^{2m}}{(2m)!}\frac{\partial^{2m} f_0}{\partial x^{2m}}\beta^m. \tag{35}$$

If we write $\alpha = \frac{a}{h_0}$, the boundary conditions at the surface (12), under the normalised variables, become:

$$\left.\begin{aligned} \eta_t + \alpha\varphi_x\eta_x - \frac{1}{\beta}\varphi_Y = 0 \\ \eta + \eta_t + \frac{1}{2}\alpha\varphi_x^2 + \frac{1}{2}\frac{\alpha}{\beta}\varphi_Y^2 = 0 \end{aligned}\right\} Y = 1 + \alpha\eta. \tag{36}$$

If we substitute the expression for φ in these boundary conditions (36) we get:

$$\begin{aligned} \eta_t + ((1+\alpha\eta)f_x)_x - (\frac{1}{6}(1+\alpha\eta)^3 f_{xxxx} + \frac{1}{2}\alpha(1+\alpha\eta)^2\eta_x f_{xxx})\beta + O(\beta^2) = 0 \\ \eta + f_t + \frac{1}{2}\alpha f_x^2 - \frac{1}{2}(1+\alpha\eta)^2(f_{xxt} + \alpha f_x f_{xxx} - \alpha f_{xx}^2)\beta + O(\beta^2) = 0. \end{aligned}$$

We can drop all terms in β and differentiate the second equation with respect to x, to obtain the shallow water equations derived earlier:

$$\begin{aligned} \eta_t + ((1+\alpha\eta)w)_x = 0 \\ w_t + \alpha w w_x + \eta_x = 0, \qquad w = f_x. \end{aligned}$$

A higher order approximation can be obtained by keeping powers of β but dropping terms of order $\alpha\beta$. This gives:

$$\begin{aligned} \eta_t + (1+\alpha\eta)w)_x - \frac{1}{6}\beta w_{xxx} + O(\alpha\beta, \beta^2) \\ w_t + \alpha w w_x + \eta_x - \frac{1}{2}\beta w_{xxt} + O(\alpha\beta, \beta^2), \qquad w = f_x. \end{aligned}$$

To get an expression in terms of η and u, instead of η and w, we expand φ_x to first order in β to get:

$$\varphi_x = w - \beta\frac{Y^2}{2}w_{xx} + O(\beta^2).$$

Taking $u = \frac{1}{1+\alpha\eta}\int_0^{1+\alpha\eta}\varphi_x$, we obtain:

$$u = w - \frac{1}{6}\beta w_{xx} + O(\alpha\beta, \beta^2),$$

thus we can write:

$$w = u + \frac{1}{6}\beta u_{xx} + O(\alpha\beta, \beta^2).$$

Plugging this into the equations found above gives:

$$\begin{aligned} \eta_t + ((1+\alpha\eta)u)_x + O(\alpha\beta, \beta^2) \\ u_t + \alpha u u_x + \eta_x - \frac{1}{3}\beta u_{xxt} + O(\alpha\beta, \beta^2). \end{aligned} \tag{37}$$

The first equations in lowest order says: $u_x = -\eta_t + O(\alpha, \beta)$. We can plug this into the $\frac{1}{3}\beta u_{xxt}$ term, since any term of $O(\alpha, \beta)$ becomes a term of order β^2 or $\alpha\beta$. Using this, equation (37) is equal to:

$$\begin{aligned} \eta_t + ((1+\alpha\eta)u)_x + O(\alpha\beta, \beta^2) = 0 \\ u_t + \alpha u u_x + \eta_x + \frac{1}{3}\beta\eta_{xtt} + O(\alpha\beta, \beta^2) = 0, \end{aligned} \tag{38}$$

which are the Bousinesq equations. Note that, due to $u_x = -\eta_t + O(\alpha, \beta)$, this is also equivalent to:

$$\begin{aligned} \eta_t + ((1+\alpha\eta)u)_x + O(\alpha\beta, \beta^2) = 0 \\ u_t + \alpha u u_x + \eta_x + \frac{1}{3}\beta\eta_{xxx} + O(\alpha\beta, \beta^2) = 0. \end{aligned} \tag{39}$$

Using the approximation: $\alpha << 1$ and eliminating u this becomes:

$$\eta_{tt} - \eta_{xx} - \frac{1}{3}\beta\eta_{xxxx} = 0.$$

In terms of the non-normalised variables, this gives us the following dispersion relation:

$$\omega^2 = c_0^2\kappa^2 - \frac{1}{3}c_0^2 h_0^2 \kappa^4$$

Which agrees with the dispersion relation $\omega^2 = g\kappa \tanh \kappa h_0$ found earlier, up to terms of order $\frac{h_0^2}{l^2}$

Now we can derive the KdV-equation in the same way, by limiting the equation to waves moving from left to right. If we look at the shallow water equation defined above, and neglect the terms of order α we have:

$$\begin{aligned} \eta_t + w_x = 0 \\ w_t + \eta_x = 0, \qquad w = f_x, \end{aligned} \tag{40}$$

which gives, just as earlier, the wave equation: $\eta_{tt} = \eta_{xx}$. Restricted to a single direction this becomes: $\eta_t = -\eta_x$, which implies $\eta = w$.

If we look for a correction to first order in α and β we can write:

$$w = \eta + \alpha A + \beta B + O(\alpha^2, \beta^2).$$

Plugging this into equation 40 gives:

$$\begin{aligned} \eta_t + \eta_x + \alpha(A_x + 2\eta\eta_x) + \beta(B_x - \frac{1}{6}\eta_{xxx}) + O(\alpha^2, \beta^2) = 0 \\ \eta_t + \eta_x + \alpha(A_t + \eta\eta_x) + \beta(B_t - \frac{1}{2}\eta_{xxt}) + O(\alpha^2, \beta^2) = 0. \end{aligned}$$

Now for terms of order α or β we can use: $\eta_t = -\eta_x + O(\alpha, \beta)$. Subtracting the second from the first equation and using the identity given above we obtain:

$$\alpha(2A_x + \eta\eta_x) + \beta(2B_x - \frac{2}{3}\eta_{xxx}).$$

From this follows:

$$A = -\frac{1}{4}\eta^2, \qquad B = \frac{1}{3}\eta_{xx}.$$

Plugging this into either of the two equations above gives:

$$\eta_t + (1 + \frac{3}{2}\alpha\eta)\eta_x + \frac{1}{6}\beta\eta_{xxx} = 0. \tag{41}$$

This is the normalised version of the KdV-equation. A big difference between the KdV-equation and the Boussinesq equation, is that the Boussinesq equation has to be solved for both η and u, whereas the KdV-equation only has to be solved for η. This is the case, since the horizontal velocity, u, has been chosen to be in a fixed direction and to be in agreement with η. By doing so we made the KdV-equation unidirectional. However, this also means that the KdV-equation only describes systems where the initial condition on both the velocity, u, and the surface, η, are in agreement. This largely limits the number of situations the KdV-equation can be applied to. However, due to the fact that analytic solutions are possible, it is still a very useful equation, which is able to predict behaviour observed in solitons, as shown in the following section:

3 Solution of the KdV-equation

This section is mostly based on M. Tabor's Chaos and integrability in nonlinear dynamics, Chapter 7 [2] *and Whithams's Linear and Nonlinear Waves* [1]

In the last section we derived the normalised version of the KdV-equation to be:

$$\eta_t + (1 + \frac{3}{2}\alpha\eta)\eta_x + \frac{1}{6}\beta\eta_{xxx} = 0.$$

We can define a new variable: $u = 1 + \frac{3}{2}\alpha\eta$ (Here u does not stand for velocity!) and replace t by $\frac{t}{6}$. Under these changes the KdV-equation becomes:

$$u_t - 6uu_x + u_{xxx} = 0. \tag{42}$$

For relatively nice waves, u_{xxx} will be small. The equation above then simplifies to: $u_t - 6uu_x$. Using the characteristics method we can study this nonlinear equation. Say: $u(s) = u(x(s), t(s))$, then $u_s = u_x x_s + t_s u_t$, now take $t_s = 1$ and $x_s = -6u$, then $u_s = 0$. From this it follows that:

$$u(s) = u_0(x) \tag{43}$$
$$t(s) = s \tag{44}$$
$$x(s) = -6su_0(x), \tag{45}$$

where $u_0(x) = u(x, 0)$ is the initial condition. Now the characteristics s are straight lines in the x, y-plane, with slopes proportional to u_0. Therefore, if there is some kind of height difference, the characteristics cross. This leads to a steepening of the wave at the front. Which means that the term u_{xxx} comes into play. For small amplitudes, the equation linearises to: $u_t + u_{xxx}$. This is a wave equation with dispersion relation: $\omega(\kappa) = \kappa^3$ which means that waves with a higher wavelength go faster. As a result waves spread out. If for certain initial conditions these two effects balance out, a stable wave appears, which travels faster than the surrounding waves. This wave is a soliton. We can try to solve it by assuming a right-traveling wave solution: $u(x, t) = f(x - ct) = f(z)$ then:

$$f_{zzz} - 6ff_z - cf_z = 0.$$

Integration with respect to z gives us:

$$f_{zz} - 3f^2 - cf + d = 0.$$

Multiplying by f_z and integrating gives:

$$f_z^2 = 2f^3 + cf^2 + 2df + e.$$

Using the following boundary conditions: $f, f_z, f_{zz} \to 0$ for $z \to \infty$ we find $d, e = 0$ and hence:

$$f_z = f\sqrt{2f + c}.$$

Dividing by the right side and integrating then gives:

$$z - z_0 = \int \frac{df}{f\sqrt{2f+c}}.$$

We can solve this integral using the following steps:
Firstly, split up the integral:

$$\begin{aligned}\int \frac{df}{f\sqrt{2f+c}} &= \frac{1}{c}\int \frac{\sqrt{2f+c}}{f}df - \frac{1}{c}\int \frac{2}{\sqrt{2f+c}} \\ &= \frac{1}{c}\int \frac{\sqrt{2f+c}}{f}df - \frac{2}{c}\sqrt{2f+c}.\end{aligned}$$

Using the substitution: $u = \sqrt{2f+c}$ we can solve the other integral:

$$\begin{aligned}\frac{1}{c}\int \frac{\sqrt{2f+c}}{f}df &= \frac{1}{c}\int \frac{2u^2}{u^2-c}du \\ &= \frac{2u}{c} + \int \frac{2}{u^2-c} = \frac{2u}{c} - \frac{2\tanh^{-1}(\frac{u}{\sqrt{c}})}{\sqrt{c}}.\end{aligned}$$

Henceforth:

$$z - z_0 = -\frac{2\tanh^{-1}(\frac{\sqrt{2f+c}}{\sqrt{c}})}{\sqrt{c}},$$

and thus:

$$\begin{aligned}\tanh^2(\frac{\sqrt{c}}{2}(z-z_0)) &= 1 + \frac{2f}{c} \\ \implies f &= -\frac{c}{2}\operatorname{sech}^2(\frac{\sqrt{c}}{2}(z-z_0)).\end{aligned}$$

So a solution for the KdV-equation is a sech^2, which has a lump like shape. This is only one family of solutions however, and since the KdV-equation is nonlinear we cannot use linear combinations to find more solutions. There is however an elegant way to find more complete solutions to this equation using the inverse scattering transform.

3.1 Inverse Scatterring Transform

The inverse scattering transform is a method to solve the KdV-equation for certain initial values. The inverse scattering transform uses quantum mechanical principles to solve an equation. It does this in the following way: Firstly, the initial wave shape $u(x,0)$ is seen as a potential in the time-independent Schrödinger equation, then the scattering data of that potential is calculated. This scattering data can be tranformed in a way corresponding to the KdV-equation, and the new scattering data can be used to calculate the corresponding potential $u(x,t)$ in certain situations.

A certain potential can support both bound and free states. Since $u(x,0)$ will be a wave, we can assume that it is zero at its limits, and hence the bound states will refer to 'negative' energy. The bound states will admit a discrete set of eigenvalues: $\lambda_n = -k_n^2$ corresponding to eigenfunctions: $\psi_n(x)$. so:

$$\psi_{n,xx} - (u_0(x) + k_n^2)\psi_n = 0. \tag{46}$$

Since u_0 goes to zero as x goes to $\pm\infty$, we need:

$$\lim_{x\to\pm\infty} \psi_n(x) \sim e^{\mp k_n x}. \tag{47}$$

When we multiply a eigenfunction $\psi_n(x)$ by a constant, it is still an eigenfunction. Therefore we can choose $\psi_n(x)$ to be the eigenfunction, corresponding to the eigenvalue $-k_n^2$, such that:

$$\lim_{x\to\infty} \psi_n(x) = e^{-k_n x}.$$

We then define define the quantity c_n as:

$$c_n = \left[\int_{-\infty}^{\infty} \psi_n^2 dx \right]^{-1} \tag{48}$$

For positive energies, the eigenvalues are a continuous spectrum with eigenvalues: $\lambda = k^2$, in the limit $x \to \infty$ we get the following solutions:

$$\lim_{x\to\infty} \Psi(x) = e^{-ikx} + b(k)e^{ikx}, \tag{49}$$

where e^{-ikx} represents an incoming wave and $b(k)e^{ikx}$ represents a reflected wave, with $b(k)$ the reflection coefficients as a function of k. In the other limit ($x \to -\infty$) we get:

$$\lim_{x\to-\infty} \Psi(x) = a(k)e^{-ikx}, \tag{50}$$

the transmitted wave travelling to the left, with transmission coefficient: $a(k)$

Now we can define the following quantity:

$$B(\xi) = \sum_{n=1}^{N} c_n e^{-k_n \xi} + \frac{1}{2\pi} \int_{-\infty}^{\infty} b(k) e^{ik\xi} dk, \tag{51}$$

which combines the data for the bound states and the data for the scattering states. Note that $a(k)^2 + b(k)^2 = 1$, therefore $b(k)$ determines $a(k)$ up to a phase-factor.

It is possible to determine an unknown potential $u(x)$ when you have the corresponding scattering data. This can be done by solving the Gelfand-Levitan-Marchenko[1] equation for K:

[1] See appendix for a derivation

$$K(x,y) + B(x+y) + \int_x^\infty B(y+z)K(x,z)dz = 0. \tag{52}$$

From this K, we can determine the corresponding potential u in the following way:

$$u(x) = -2\frac{d}{dx}K(x,x). \tag{53}$$

In order to solve the KdV-equation we need to do two different things. Firstly, we need to determine how the scattering data evolves under the KdV-equation. Secondly, we need to solve equation (52).

We will start by figuring out what happens with the scattering data when we transform it. The KdV-equation is given by:

$$u_t - 6uu_x + u_{xxx} = 0. \tag{54}$$

Note that although the parameter t represents time in the KdV-equation, we shoud not see this t as time in the Schrödinger equation, but more as a deformation parameter. This means that we can apply a t dependence to the time independent eigenvalue λ and wave function Ψ. So the time-independent Schrödinger equation then becomes:

$$\Psi_{xx} - (u(x,t) - \lambda(t))\Psi = 0 \tag{55}$$

Now we can express u in terms of Ψ in the following way:

$$u = \frac{\Psi_{xx}}{\Psi} + \lambda, \tag{56}$$

(If $\Psi = 0$ then $\Psi_{xx} = 0$ as well) substituting this into the KdV-equation gives us(after some manipulations):

$$\Psi^2\frac{d\lambda}{dt} + \frac{\partial}{\partial x}(\Psi Q_x - \Psi_x Q) = 0, \tag{57}$$

where Q is given by:

$$Q = \Psi_t + \Psi_{xxx} - 3(u+\lambda)\Psi_x$$

.

Since we are looking at waves, we can assume: $u \to 0$ when $|x| \to \infty$, as we did earlier. For the bound states ψ_n we then have:

$$\int_{-\infty}^\infty \psi_n^2 dx = c_n^{-1} > 0.$$

Therefore integrating (57) gives:

$$c_n\frac{d\lambda}{dt} = \int_{-\infty}^\infty \frac{\partial}{\partial x}(\Psi Q_x - \Psi_x Q)dx = 0. \tag{58}$$

From which we can conclude that λ is independent of t.

For the scattering states we can look at a certain eigenvalue λ and let it be independent of t. So in both the bound and scattering states we find:

$$\frac{\partial}{\partial x}(\Psi Q_x - \psi_x Q) = 0, \tag{59}$$

and thus:

$$Q \equiv \Psi_t + \Psi_{xxx} - 3(u+\lambda)\Psi_x = C\Psi, \tag{60}$$

with C independent of x (but not of t).

We can write $\lambda = \mu^2$, (with $\mu = ik_n$ for bound states). Our boundary conditions state that for all t we have $u = 0$ and thus $\Psi = Ae^{i\mu x}$ when $x \to \infty$. Furthermore, we know that λ is independent of the parameter t. Using this and equation (60) we get: $C = -4i\mu^3$. Plugging this value for C into (60) we obtain:

$$\Psi_{xx} + (\mu^2 - u)\Psi = 0 \tag{61}$$

$$\Psi_t + \Psi_{xxx} - 3(u+\lambda)\Psi_x + 4i\mu^3\Psi = 0. \tag{62}$$

We want to use these equations to find out how the scattering data changes. We already know that $\lambda_t = 0$, so that stays the same. For the bound states we have: $c_n^{-1} = \int_{-\infty}^{\infty} \psi_n^2 dx$ and thus, using equation 62:

$$\frac{d}{dt}\int_{-\infty}^{\infty} \psi^2 dx = \int_{-\infty}^{\infty} 2\psi\psi_t dx =$$

$$\int_{-\infty}^{\infty} (-2\psi\psi_{xxx} + 6(u+\mu^2)\psi_x\psi - 8i\mu^3\psi^2)dx =$$

$$\int_{-\infty}^{\infty} (-2\psi\psi_{xxx} + 6\mu^2\psi_x\psi + 6u\psi_x\psi)dx - 8i\mu^3\int_{-\infty}^{\infty}\psi^2 dx$$

If we then use equation 61 to write $u\psi = \psi_{xx} + \mu^2\psi$ we get:

$$\frac{d}{dt}\int_{-\infty}^{\infty} \psi^2 dx = \int_{-\infty}^{\infty} (-2\psi\psi_{xxx} + 12\mu^2\psi_x\psi + 6\psi_{xx}\psi_x)dx - 8i\mu^3\int_{-\infty}^{\infty}\psi^2 dx$$

$$= \big[-2\psi\psi_{xx} + 4\psi_x^2 + 6\mu^2\psi^2\big]_{-\infty}^{\infty} - 8iu^3\int_{-\infty}^{\infty}\psi^2 dx = -8i\mu^3\int_{-\infty}^{\infty}\psi^2 dx \tag{63}$$

Since $\mu = ik_n$ it follows that:

$$c_n(t) = c_n(0)e^{8k_n^3 t} \tag{64}$$

The reflection coefficient can be calculated in a similar way. We are looking for a scattering state wave function at a time t: $\Psi = f(k,t)e^{-ikx} + g(k,t)e^{ikx}, \quad x \to \infty$. If we plug this into equation (62), with $u = 0$, for we are working in the limit: $x \to \infty$, then we get:

$$f_t e^{-ikx} + 8k^3 i f e^{-ikx} + g_t e^{ikx} = 0.$$

So:

$$f(k,t) = e^{-8ik^3 t}, \qquad g(k,t) = \beta(k),$$

which tells us that the reflection coefficient $b(k,0)$ changes as:

$$b(k,t) = b(k,0)e^{8ik^3 t}. \tag{65}$$

So now we know how k_n, c_n and $b(k)$ change in time. To find the potential corresponding to this data, we need to solve equation (52).

First we note that when a potential is reflectionless, equation 52 simplifies to:

$$K(x,y) = -\sum_{n=1}^{N} c_n(0)e^{8k_n^3 t - k_n(x+y)} - \sum_{n=1}^{N} c_n(0)e^{8k_n^3 t - k_n(x)} \int_{-\infty}^{\infty} e^{k_n z} K(z,y)dz. \tag{66}$$

Now we may assume that the solution is of the form:

$$K(x,y) = \sum p_n(x,t)e^{-k_n y}, \tag{67}$$

i.e, the y-dependence in $K(x,y)$ is the same as in $B(x+y)$. Writing $g_n = c_n(0)e^{8k_n^3 t - k_n x}$ we get the equation:

$$\sum_{n=1}^{N} \Big(p_n(x,t) + g_n(x,t) + \sum_{m=1}^{N} \int_x^{\infty} g_n(z)p_m(x)e^{-k_m z}dz \Big) e^{-k_n y} = 0. \tag{68}$$

Since this holds for all values of y, we need:

$$p_n(x,t) + g_n(x,t) + \sum_{m=1}^{N} \int_x^{\infty} g_n(z)p_m(x)e^{-k_m z}dz = 0, \qquad \forall n. \tag{69}$$

We can see p_n and g_n as components of column vectors, by doing so we can write the equation above as:

$$P(x)p(x) + g(x) = 0, \tag{70}$$

where $P(x)$ is the matrix given by

$$P_{mn}(x) = \delta_{mn} + \int_x^{\infty} g_m(z)e^{-k_n z}dz.$$

Saying h is the row vector given by: $h_n = e^{-k_n x}$, we get

K(x,x) = h(x)·$p(x) = -h(x) \cdot P^{-1}(x)g(x)$.Since

$$\frac{d}{dx}P_{mn}(x) = -g_m(x)e^{-k_n x} = -g_m(x)h_n(x), \tag{71}$$

which is the matrix where the n^{th} row is given by: $g_n h$. From this it follows that $P^{-1}\frac{dP}{dx}$ is the matrix where every element is given by:

$$(P^{-1}\frac{dP}{dx})_{mn} = (P^{-1}g)_m h_n, \tag{72}$$

and therefore:

$$K(x,x) = Tr(P^{-1}\frac{dP}{dx}) = \frac{1}{|P|}\frac{d}{dx}|P|, \tag{73}$$

with $|P|$ the determinant of the matrix P.
So now we have:

$$u = -2\frac{d}{dx}K(x,x) = -2\frac{d^2}{dx^2}log(|P|). \tag{74}$$

If we do this for $n = 2$ for example, we get the following matrix P.

$$\begin{pmatrix} 1 + \frac{c_1(0)e^{8k_1^3 t - 2k_1 x}}{2k_1} & \frac{c_1(0)e^{8k_1^3 t-(k_1+k_2)x}}{k_1+k_2} \\ \frac{c_2(0)e^{8k_2^3 t-(k_1+k_2)x}}{k_1+k_2} & 1 + \frac{c_2(0)e^{8k_2^3 t-2k_2 x}}{2k_2} \end{pmatrix}$$

We can use this to determine what happens for reflectionless initial conditions, with two bound states. Such an initial condition is: $u(x,0) = -6\,\mathrm{sech}^2(x)$. The bound states are then given by:

$$\psi_1 = \frac{1}{4}\,\mathrm{sech}^2(x), \qquad k_1 = 2 \text{ and } c_1(0) = 12 \tag{75}$$

$$\psi_2 = \frac{1}{2}\tanh(x)\,\mathrm{sech}(x), \qquad k_2 = 1 \text{ and } c_2(0) = 6. \tag{76}$$

By using equation 73 we get:

$$\begin{aligned} K(x,x;t) &= \frac{-12e^{64t-4x} - 6e^{8t-2x} - 6e^{72t-6x}}{1 + 3e^{64t-4x} + 3e^{8t-2x} + e^{72t-6x}} \\ &= \frac{-3(2e^{28t-x} + e^{36t-3x} + e^{-24t+x})}{3\cosh(x-28t) + \cosh(3x-36t)}, \end{aligned}$$

and from (74):

$$u(x,t) = -\frac{12(3 + 4\cosh(2x-8t) + \cosh(4x-64t)}{(3\cosh(x-28t) + \cosh(3x-36t))^2}. \tag{77}$$

Introducing the variables: $x_1 = x - 4k_1^2 t = x - 16t$ and $x_2 = x - 4k_2^2 t = x - 4t$ transforms this into:

$$u(x,t) = -\frac{12(3 + 4\cosh(2x_1 + 24t) + \cosh(4x_1)}{(3\cosh(x_1 - 12t) + \cosh(3x_1 + 12t))^2}. \tag{78}$$

Taking the limit $t \to \infty$ then gives:

$$\begin{aligned}\lim_{t\to\infty} u(x,t) &\approx \frac{-32}{((1/\sqrt{3})e^{2x_1} + \sqrt{3}e^{-2x_1})^2} \\ &= \frac{-32}{(e^{2x_1 - \ln\sqrt{3}} + e^{-2x_1 + \ln\sqrt{3}})^2} \\ &= -8\,\mathrm{sech}^2(2x_1 + \ln\sqrt{3}).\end{aligned}$$

Doing the same for x_2 gives:

$$\lim_{t\to\infty} u(x,t) = -2\,\mathrm{sech}^2(x_2 - \ln\sqrt{3}).$$

Similarly, it can be shown that in the limit $t \to \pm\infty$ for either fixed x_1 or x_2, $u(x,t)$ behaves as:

$$\lim_{t\to\pm\infty} u(x,t) = -2\,\mathrm{sech}^2(x_2 \pm \ln\sqrt{3}) - 8\,\mathrm{sech}^2(2x_1 \mp \ln\sqrt{3}). \tag{79}$$

This shows two waves that overtake each other at $t = 0$, and then continue on without their shapes being changed. The only result of the interaction is the small phase shift $\ln\sqrt{3}$.

More generally, for any potential of the form $u(x,0) = V\,\mathrm{sech}^2 x$, with N bound states, with eigenvalues $\lambda_n = -k_n^2$, the solutions behave in the limits as:

$$\lim_{t\to\pm\infty} u(x,t) = \sum_{n=1}^{N} -2\lambda_n^2\,\mathrm{sech}^2(k_n(x - 4k_n^2 t - \delta_n)), \tag{80}$$

with the phase shift δ_n given by:

$$\delta_n = \frac{1}{2k_n}\ln\Big\{\frac{c_n(0)}{2k_n}\prod_{m=1}^{N-1}\Big(\frac{k_n - k_m}{k_n + k_m}\Big)^2\Big\}.$$

This shows a train of solitons, with the biggest at the front and the smallest in the rear, with the only effect of the interaction a small phase difference.

More generally, it can be shown that, for any initial condition, the number and size of solitons that appear can be found by looking at the bound state eigenvalues of the Schrödinger equation with the potential given by this initial condition. For initial conditions with $b(k) \neq 0$ the solution will also contain a dispersive part that is not a soliton, a solution for this has not been found yet. However, due to the dispersive character of this part of the solution and the fact that solitons travel faster than the small dispersive waves, for $\lim_{t\to\infty}$ the solution is a train of solitary waves, corresponding to the bound states only.

4 Experiments

Earlier experiments on counter propagating solitary waves by W. Craig, P. Guyenne, J. Hammack, D. Henderson and C. Sulem [3] and T. Maxworthy [4], showed that head-on collisions between solitons are not fully elastic. The amplitude of the soliton is slightly smaller after collision than before, furthermore a phase-lag occurs for both solitons. This is in agreement with numerical results by Cooker, Weidman and Bale [5], W. Craig, P. Guyenne, J. Hammack, D. Henderson and C. Sulem [3]. Due to the loss of amplitude and thus speed of the solitons after collision, the definition of the phase-lag in this situation is not immediately clear. The definition can be given in the following way. Let the path of a soliton before the collision be given by: $ct + a$ and after by: $c^+t + a^+$. Furthermore, let τ be the time for which the variation of the following quantity is minimal:

$$V(t) = \int (x - \frac{C}{M})^2 \eta dx \tag{81}$$

Here $\frac{C}{M}$ is the center of gravity of our system. Heuristically, this is the point where the combined soliton is at its most peaked. Then the phase-lag is given by: $(a - a^+ + \tau(c - c^+))$.[3] Maxworthy [4] also did an experiment on soliton reflection at a vertical wall. The value found here was in exact agreement with the analytical result found by H. Power and A. T. Chwang [6]. I did similar experiments on both collisions and reflections of solitons, to compare them to these results.

4.1 Experimental set-up

A watertank of 2.4 meters in length was used for the experiments. On the side of the tank there was a container, with a slide-door, which could be used to release water into the tank. Opening the slide door creates a train of solitary waves and some small extra waves. Depending on the amount of water added to the system and the speed with which the slide-door was opened, it is possible to create a single solitary wave with very little noise. A camera was used to film the container, and MATLAB was used to analyse the video; to get data on the shape and movement of the waves. This was done by converting frames from the video to grayscale, and then selecting pixels above a certain threshold value. After this all pixels that where not part of the wave were manually deleted. The resulting image was the watersurface with some holes, these holes where filled up by fitting a straightline between nearest known points of the watersurface. Firstly, the experiment was carried out on a single solitary wave. Of many attempts, the two with least noise where used to gather the data. From this data I firstly determined whether the observed solitary wave behaved like a soliton, as predicted by the theory. I then measured what happened at the reflection. This was done by determining the trajectory of the soliton both before and after reflection, from this I determined point of intersection. When there is no delay at reflection, this point should be at the exact boundary of the tank. Finally, the experiment was carried out with two solitary waves, this was done by refilling the container after the first wave was created and then releasing the water again creating a second solitary wave, which then collided head-on with the

Figure 1: Experimental set-up

reflected first soliton. The trajectory of these solitons was determined before and after collision, similar to what has been done by W. Craig, P. Guyenne, J. Hammack, D. Henderson and C. Sulem [3].

4.2 Verification

Firstly, I analysed the wave shape created by releasing water into the tank, to see if this behaved similar to solitons as predicted by the theory. A soliton as predicted by the KdV-equation has the property that the amplitude, width, and speed all depend on the same variable. For the wave observed in the experiment to be a KdV-soliton we need it to be similar to the following function:[1]

$$\eta = \eta_0 \operatorname{sech}^2((\frac{3\eta_0}{4h_0^3})^{\frac{1}{2}}(x - Ut)) \qquad U = \sqrt{(}g(h + \eta)) \tag{82}$$

Fitting this through the data obtained from the video analysis I got the following results: figure 2 when the width and amplitude are both determined independently, and figure 3 when the width was taken to be dependent on the amplitude. When time-dependence was taken into account: figures 4, 5. In both fits the amplitude and width are dependent on each other but the speed is determined independently. The parameter d states the difference between the measured speed, and the speed predicted by: $\sqrt{g(h+\eta)}$ figure 4 shows the soliton before the first collision and figure 5 after the first collision. In these figures it seems that the observed waves match the theory well. The only structural difference that seems to occur, is that the measured solitons seem

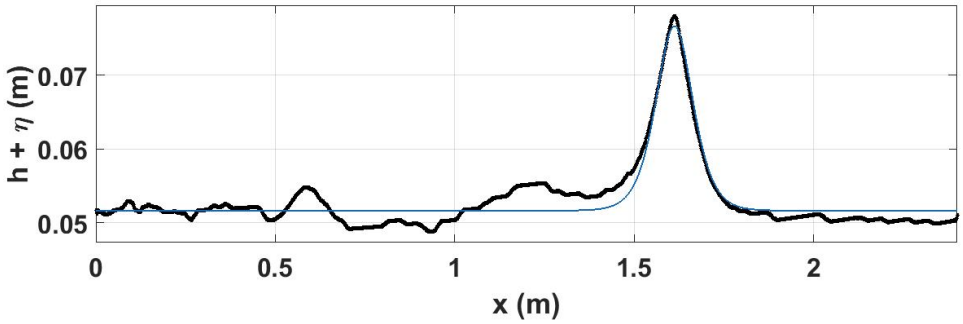

Figure 2: $h + \eta\,\mathrm{sech}^2(\sqrt{c}(x - x_0))$ with $h = 0.0516, \eta = 0.0251$ and $c = 211.4$

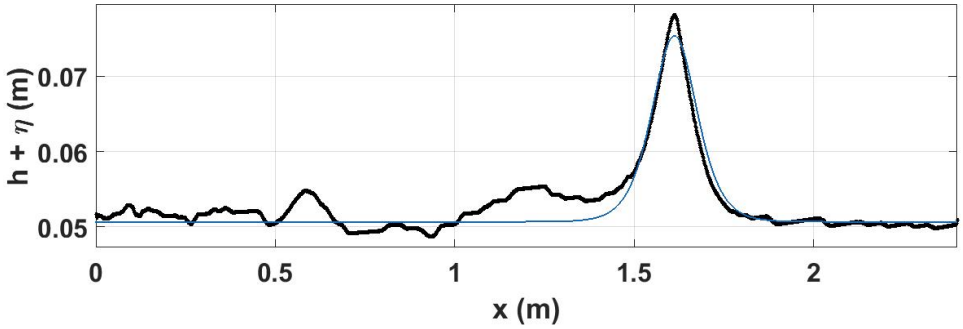

Figure 3: $h + \eta\,\mathrm{sech}^2(\sqrt{\frac{3\eta}{4h^3}}(x - x_0)$ with $h = 0.0507, \eta = 0.0246$

slightly higher with respect to to their width, compared with the theoretical predictions. However the match seems good enough to assume the waves created by this set-up are indeed KdV-solitons.

4.3 Head-on Collisions

The trajectories $(ct + a)$ of two solitons were as follows: (with c in $\frac{m}{s}$ and a in meters, and with $t = 0$ for the collision point defined earlier.)

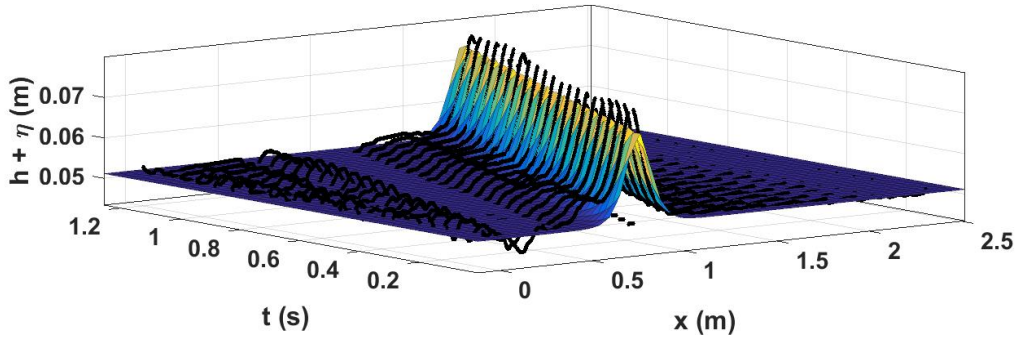

Figure 4: $h+\eta\,\mathrm{sech}^2(\sqrt{\frac{3\eta}{4h^3}}(x-x_0-(\sqrt{g(h+\eta)}+d)t)$ with $h=0.0512, \eta=0.0227, d=0.0045$

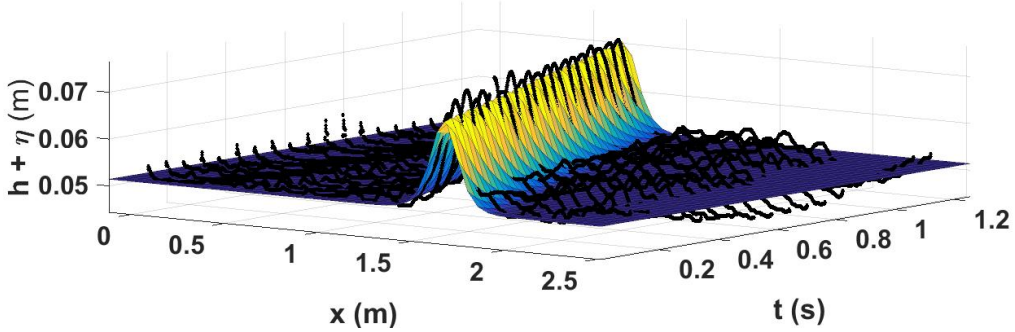

Figure 5: $h+\eta\,\mathrm{sech}^2(\sqrt{\frac{3\eta}{4h^3}}(x-x_0+(\sqrt{g(h+\eta)}+d)t)$ with $h=0.0514, \eta=0.0193, d=-0.024$

Collision 1:	
Soliton 1	$Before : 0.6394t + 1.526(\pm 0.02, \pm 0.017)$
	$After : 0.735t + 1.508(\pm 0.008, \pm 0.007)$
Soliton 2	$Before : -0.707t + 1.391(\pm 0.007, \pm 0.006)$
	$After : -0.7575t + 1.409(\pm 0.01, \pm 0.009)$
Collision 2:	
Soliton 2	$Before : 0.7637t + 1.068(\pm 0.03, \pm 0.024)$
	$After : 0.7373t + 1.037(\pm 0.016, \pm 0.014)$
Collision 3:	
Soliton 1	$Before : 0.6523t + 1.34(\pm 0.025, \pm 0.022)$
	$After : 0.7501t + 1.373(\pm 0.055, \pm 0.05)$
Soliton 2	$Before : -0.6419t + 1.475(\pm 0.02, \pm 0.017)$
	$After : -0.7135t + 1.448(\pm 0.013, \pm 0.017)$

In these measurements, the speed of the solitons does not seem to be very stable. The solitons seem to go either faster or slower after both reflection and collision. In the numerical simulations done by W. Craig, P. Guyenne, J. Hammack, D. Henderson and C. Sulem [3] they found that when two solitons of relative amplitudes: $\eta_1/h = 0.4$ and $\eta_2/h = 0.3$ collided head on, the amplitudes after collision were respectively: $\eta_1/h = 0.3987$ and $\eta_2/h = 0.2983$. This difference is very small, and should not change the velocity of the soliton in any measurable way. The phase-lag that was determined by these numerical simulations was equal to: $0.3021h$ and $0.3223h$, which for a depth of 5 centimeters comes down to approximately 1.5 centimeters. For relatively smaller waves, a smaller phase-lag is expected. If we look at the difference between the trajectories before and after collision at $t = 0$ we get the following values:

Collision 1: (figure 6)	
Soliton 1	0.018
Soliton 2	− 0.018
Collision 2: (figure 7)	
Soliton 2	0.031
Collision 3: (figure 8)	
Soliton 1	− 0.029
Soliton 2	0.027

With standard deviations of respectively: $0.018, 0.11, 0.28, 0.055, 0.024$. From this all we can only conclude, that with the methods used, the phase-lag does not differ measurably from zero.

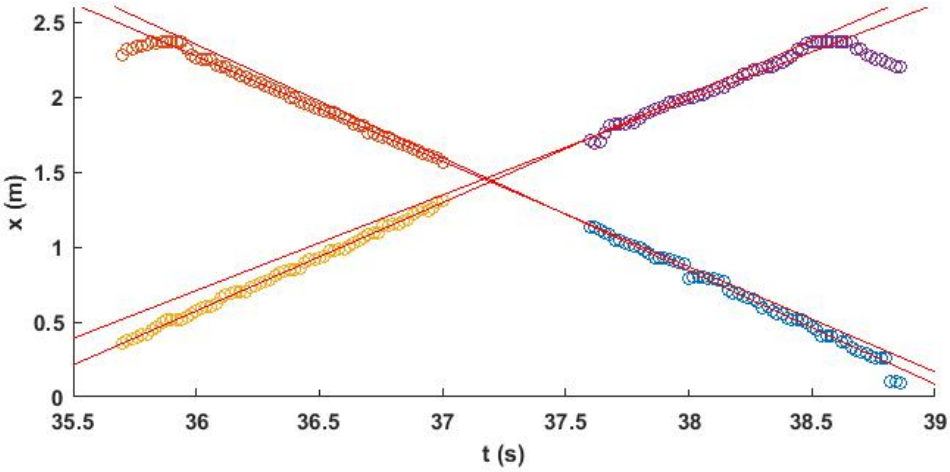

Figure 6: Collision 1

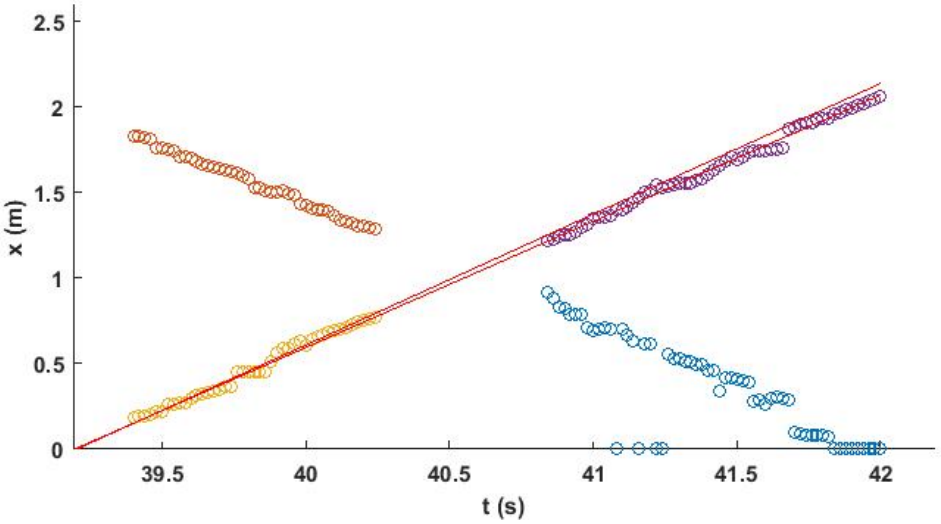

Figure 7: Collision 2

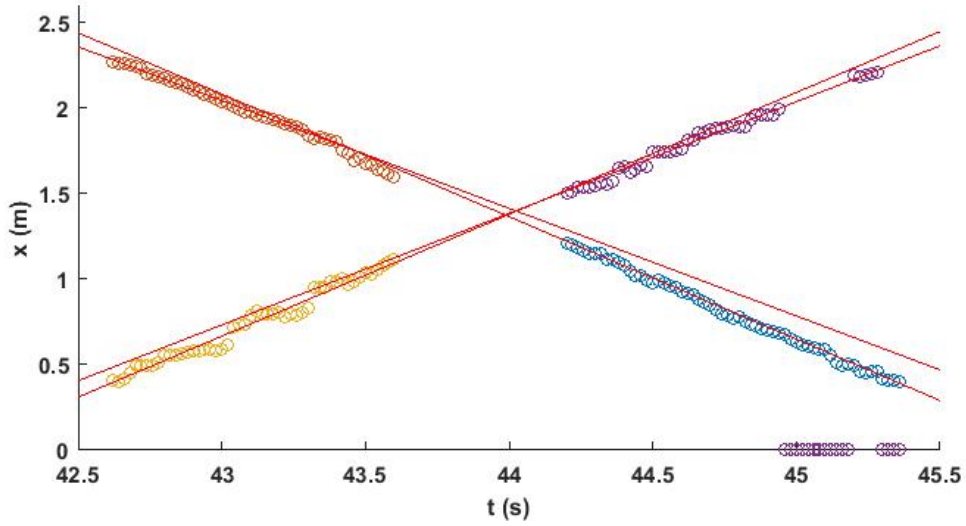

Figure 8: Collision 3

4.4 Experiments Reflection

4.4.1 Video 1

For the first video, the reflection at the left side was measured three times. The video that was used had 30 frames per second and a resolution of 506x659. Using MATLAB to determine the trajectories ($t = \frac{1}{c}x + a$) of the center of gravity of the soliton,the following results were obtained before and after three different reflections:

$$\begin{aligned} 1) -0.1062x + 56.44(\pm 0.0013, \pm 0.85) \\ 0.1056x + 54.84(\pm 0.0023, \pm 0.75) \\ 2) -0.1070x + 195.9(\pm 0.0016, \pm 0.6) \\ 0.1096x + 193.9(\pm 0.0019, \pm 0.6) \\ 3) -0.1102 + 338.5(\pm 0.0016, \pm 0.5) \\ 0.1043 + 337.4(\pm 0.0028, \pm 0.9) \end{aligned}$$

Estimating the standard deviation in the inverse velocity of the soliton ($\frac{1}{c}$), and assuming it stays the same gives: $\sigma = 0.0023$ with a mean inverse velocity of: 0.1072. The average difference between the constants (i.e. $a_1 - a_2$) is 1.56 with a standard deviation of 0.45. So the average point of reflection, i.e. the intersection of the trajectory before reflection, and the trajectory after reflection, based on this data is: 7.2795 with a standard deviation of 2.1. The real reflection point is at 20 which is approximately seven standard deviations from our measured value.

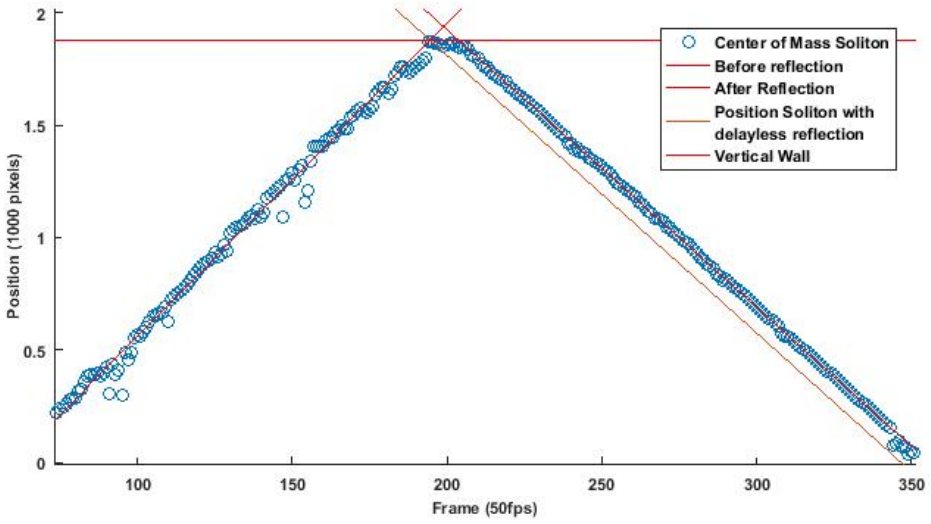

Figure 9: Reflection Soliton

4.4.2 Video 2

The second video used had a frame rate of 50 frames per second and a resolution of 1080x1920. In this video only two reflection could be effectively measured, with the following results:

$$\begin{aligned} 1) & 0.07107x + 60.73(\pm 0.0012, \pm 1.20) \\ & -0.08089x + 355.8(\pm 0.00021, \pm 0.2) \\ 2) & -0.08089x + 355.8(\pm 0.00021, \pm 0.2) \\ & 0.07519x + 367.1(\pm 0.0025, \pm 2.4) \end{aligned}$$

These give intersections at: 1944 pixels (figure 9) and -70.27 pixels, while the actual edges are at: 1880 pixels and 0 pixels. So the distance between the actual reflection point and the virtual reflection point is respectively: 64 pixels and 70.27 pixels. An estimation for the standard deviation with which these two values are determined gives: $\sigma = 9.8995$. So again the difference between the measured virtual point of reflection and the real point of reflection is more than six standard deviations.

We can compare this to results found on head-on collisions between solitons of equal amplitude, and the analytical and numerical results on reflection by H. Power and A.T. Chang. The results given above are all in pixel and frame. One pixel corresponds to 2.4/1880 metres. Therefore, the points of reflection, as measured here are: 8.2cm and 9.0cm from the real boundary. The inverse velocity of the soliton at the three intervals in meter per second is: $1.11, -1.27, 1.18$. So the time in seconds that the soliton stays at the boundary is given by: $1.11*0.082+1.27*0.082 = 0.195$ and $1.27*0.09+1.18*0.09 = 0.22$.

The analytical result for this phase lag as found by H. Power and A.T. Chang [6] is:

$$\Delta t(\frac{g}{h})^{\frac{1}{2}} = \frac{1.52}{\sqrt{\epsilon}[1 + O(\epsilon)]}$$

With $\epsilon = \frac{\eta}{h}$ the relative amplitude of the soliton. The depth h in this experiment is 0.051 meters. So $\Delta t(\frac{g}{h})^{\frac{1}{2}} = 2.73$ at the first reflection and $\Delta t(\frac{g}{h})^{\frac{1}{2}} = 3.08$ at the second reflection. The amplitude of the soliton is: 0.025 meter and declines to approximately 0.018 meters after the second reflection. So ϵ ranges between: 0.5 and 0.36, thus $\frac{1.52}{\sqrt{\epsilon}}$ ranges from 2.14 to 2.53, which is a bit lower than the theoretical result, but of the same order of magnitude.

4.5 Discussion

The measurements of the location using video gave a well defined speed in all the attempts. However, the spread in results show a far greater uncertainty. The lack of noise in the measurements suggests that these errors are not caused by random effects, and are therefore probably more structural errors, coming from either the water itself, the video recording, or the video-analysis.

By releasing the water in the tank we created both a solitary wave and a number of small waves. It might be the case that a wave corresponding to the eigenfrequency of our tank was created. This could possibly explain the apparent acceleration observed in the solitons at times. In the reflection experiment the solitons were created by adding 0.4 liters of water to our system. The solitons created this way have a height of 1.9 centimeter at a depth of 5.1 centimeters. The tank is 8.5 centimeters wide. Integrating $\eta \operatorname{sech}^2(\sqrt{\frac{3\eta}{4h^3}} * x)$ with $\eta = 0.019$ and $h = 0.05$, from -1.2 to 1.2 (i.e. the length of the tank), and multiplying the result by the width of the tank gives: 0.311 liters, which is the volume of the soliton. This means 0.089 liters are making up extra waves. Now if all this water is part of a single wave, whose wavelength is twice the wavelength of the tank, then this wave has an amplitude of 0.24 millimeters. This is very small and unlikely to explain the effects observed.

Before the wave is created the water is at rest. At this point the depth measured by the camera is about 1.25 times more shallow on the right side of the tank than at the left side. This is probably due to this point being further away from the camera. If this has a big effect on the measured speed of the soliton, we should be able to measure it. If we fit a polynomial of degree two through the trajectory of the center of mass, and thus include an acceleration term, we should be able to pick up structural differences in speed between the left and right side of the tank. The following results were obtained for the trajectory before and after reflection:

$$\text{Before reflection: } x = -0.01117t^2 - 0.843 * t.$$

Here we have chosen our trajectory, such that $x = 0$ at $t = 0$. The 95% confidence intervals of the quadratic term and linear term are given by respectively: 0.0153 and 0.0383.

After reflection: $x = -0.01004t^2 - 0.797 * t$.

The 95% confidence intervals of the quadratic term and linear term are given by respectively: 0.0027 and 0.0073.

In the first case there is no significant acceleration measured. In the second case there is a small acceleration term. The wave takes approximately three seconds to go from the right to the left side of the tank. So the difference in speed measured here between the right and left side is approximately 0.03 metres per second. This is slightly bigger than the uncertainty in the velocities found in the collision experiments. It does not explain the variation seen there though. For example: In the first and third collision, soliton 1 increases in velocity, even though it goes from left to right, and should therefore slow down according to the quadratic term found above.

If we look at the collisions themselves, we might see other reasons for the variation in velocity. Figures B.1, B.2 and B.3 show the three collisions. Here it is quite clear that there is actually quite a lot of noise. Soliton 1 which travels from left to right in the third collision speeds up significantly, however in the figure the soliton is hardly distinguishable from the noise. If we compare this to figure B.4, which shows the soliton which was analysed in the experiments on reflection, we see that the amount of noise is relatively less. Furthermore in figure B.4 the sech^2-shape of the KdV-soliton is more recognizable. On top of this the speeds measured do not seem to agree with the observed height of the solitons. Soliton two, for example, has a height of 6.5 centimetres(depth plus amplitude) before and after the first collision, which should, according to $\sqrt{g * (\eta + h)}$, correspond to a velocity of 0.8 metres per second. Which is significantly faster than the measured speed of 0.71 and 0.76. Figure B.5 shows the single soliton used for the reflection experiment, where every plot shows the soliton after another reflection. Compared to the plots of the three consecutive collisions, there is much less noise visible. Furthermore, the shape and amplitude of the soliton appear to be maintained longer and better. This seems to imply that a different way of creating solitons is necessary to measure the effect of the collision, without too much uncertainty. To get better results a longer tank could be used. The high velocity relative to the smaller waves, would mean the soliton will escape them given enough time, with the result that the actual measurement happens with less background noise.

Another thing that is clear from these figures, that doesn't agree with the numerical results of for example H. Power and C.W. Chwang [6], is the observed amplitude loss. Their results showed that reflection was elastic, but after the first reflection, the amplitude of the soliton in the experiment has gone from 2.3 to 1.9 centimeters. In the analytic estimate of the phaselag, obtained by a soliton reflecting at a vertical wall, it has been assumed the amplitude of the soliton stays the same. This might explain the difference between the observed and the theoretically predicted phaselag.

In conclusion, a phaselag can be observed when solitons reflect at a vertical wall. This situation is similar to a head-on collision between two equally sized solitons, for which the effect had already been measured. Furthermore the measurements are in agreement with the analytic and numerical results available for soliton reflection. To get

more precise and reliable results however a different method of creating solitons should be used. Both to be able to control the size of the solitons, and therefore be able to recreate the experiment, but mostly to get less distortion of small background waves.

A The Gelfand-Levitan-Marchenko equation

In this section we will derive the Gelfand-Levitan-Marchenko equation. The derivation is based on "Theory of Solitons" by S. Novikov, S. V. Manakov, L.P. Pitaevskii and V.E. Zakharov [7], and "Scaling, Mathematical Modelling, and Integrable Systems" by D.H. Sattinger [8]
In section 3.1 the Gelfand-Levitan-Marchenko equation was used to determine a potential from the scattering data. This equation is given by:

$$K(x,y) + B(x+y) + \int_x^\infty B(y+z)K(x,z)dz = 0. \tag{A.1}$$

Where B is defined as:

$$B(\xi) = \sum_{n=1}^{N} c_n e^{-\kappa_n \xi} + \frac{1}{2\pi}\int_{-\infty}^{\infty} b(k)e^{ik\xi}dk. \tag{A.2}$$

And the potential, $u(x)$, can be recovered from $K(x,x)$ in the following way:

$$u(x) = -2\frac{d}{dx}K(x,x). \tag{A.3}$$

To derive this equation we need to start with stating the Schrödinger equation:

$$-\frac{d^2\psi}{dx^2} + u(x)\psi = k^2\psi. \tag{A.4}$$

We will assume that the potential $u(x)$ goes to zero rapidly enough. When that is the case, there is only a finite amount, N, of bound states. The scattering state correspond to k on the real line, while the bound state eigenvalues are given by n points on the imaginary axis, $k = i\kappa_n$ for $n = 1, .., N$ $\kappa > 0$.

For the bound state eigenvalues $i\kappa_n$, we stated earlier that we get the following asymptotic behaviour for the eigenfunctions:

$$\psi(x) \sim e^{\mp\kappa_n x}, \quad x \to \pm\infty. \tag{A.5}$$

For a bound state, we define two eigenfunctions: ψ_n and ϕ_n. Where just as earlier:

$$\lim_{x\to\infty} \psi_n(x) = e^{-\kappa_n x}, \tag{A.6}$$

and similarly:

$$\lim_{x\to-\infty} \phi_n(x) = e^{\kappa_n x}. \tag{A.7}$$

Since both functions should fall off exponentially in both limits, they are related through:

$$\phi_n(x) = c_n'\psi_n(x). \tag{A.8}$$

The scattering data, c_n, was defined as:

$$c_n = \left[\int_{-\infty}^{\infty} \psi_n^2 dx \right]^{-1}. \tag{A.9}$$

Note that c'_n is related to c used in the scattering data by:

$$c_n = \frac{{c'_n}^2}{\int_{-\infty}^{\infty} \phi^2 dx} \tag{A.10}$$

This will be useful later on.

For real values of k, i.e. the scattering states. The solutions are found in a 2-d space. With basis elements: ψ_1, ψ_2. These basis elements have the following asymptotic behaviour:

$$\left.\begin{aligned} \psi_1(x,k) &= e^{-ikx} \\ \psi_2(x,k) &= e^{ikx} \end{aligned}\right\} \quad \lim x \to \infty$$

Another basis we can construct for the same k is given by:

$$\left.\begin{aligned} \phi_1(x,k) &= e^{-ikx} \\ \phi_2(x,k) &= e^{ikx} \end{aligned}\right\} \quad \lim x \to -\infty$$

We can transform the basis $\psi_{1,2}$ to the basis $\phi_{1,2}$ by writing it as a linear combination of the other:

$$\phi_i = \sum_{j=1,2} T_{ij}\psi_j, \quad i = 1, 2$$

Taking the limit $x \to \pm\infty$ gives the relations: $\phi_1 = \overline{\phi_2}$ and $\psi_1 = \overline{\psi_2}$. Now since the potential is real, this holds for all x. Therefore the transition matrix, T, is given by:

$$T(k) = \begin{pmatrix} a(k) & b(k) \\ \overline{a}(k) & \overline{b}(k) \end{pmatrix},$$

which means we can write: $\phi_1(x,k) = a(k)\psi_1(x,k) + b(k)\psi_2(x,k)$. Furthermore, since ϕ_2 and ψ_2 are nothing but the complex conjugates of ϕ_1 and ψ_1, we can get rid of the subscripts by writing: $\phi = \phi_1$ and $\psi = \psi_1$

For the next step it is usefull to use the Wronskian. The Wronskian of two functions is defined by: $W(f,g) = f\frac{dg}{dx} - \frac{df}{dx}g$. Therefore,

$$\frac{d}{dx}W(f,g) = f\frac{d^2g}{dx^2} - \frac{d^2f}{dx^2}g. \tag{A.11}$$

From this it is clear that $W(f,g)$ is independent of x if f and g are both solution of equation (A.4). Therefore we can analyse $W(\phi,\overline{\phi}), W(\psi,\overline{\psi})$ and $W(\phi,\overline{\psi})$ in the limit $x \to \infty$ to obtain:

$$W(\phi,\overline{\phi}) = W(\psi,\overline{\psi}) = 2ik \tag{A.12}$$

$$W(\phi, \overline{\psi}) = 2ika(k). \tag{A.13}$$

From equation (A.12) together with the relation $\phi(x,k) = a(k)\psi(x,k) + b(k)\overline{\psi}(x,k)$, we find:

$$|a(k)|^2 - |b(k)|^2 = 1.$$

Earlier, we stated that scattering solutions behaved as:

$$\begin{aligned} e^{ikx} + r(k)e^{-ikx} \qquad & x \to \infty \\ t(k)e^{ikx} \qquad & x \to -\infty. \end{aligned}$$

So it follows that: $r(k) = \frac{b(k)}{a(k)}$ and $t(k) = \frac{1}{a(k)}$. The functions $\psi(x,k)$, $\phi(x,k)$, $b(k)$ and $a(k)$ have been defined here for real values of k only. We can expand this definition to the upper half k plane, i.e. all k such that $\Im(k) > 0$, and show that these functions are analytic on this domain. It will turn out to be the case that $a(k) = 0$ if and only if k^2 is a bound state eigenvalue of the Schrödinger equation. Therefore $a(k)$ contains information on both the continuous and the discrete spectrum.

To show that this is true we start out by writing equation (A.4) as an integral equation.

$$\psi(x,k) = e^{-ikx} - \int_{-\infty}^{\infty} G(x,s,k)u(s,k)\psi(s,k)ds. \tag{A.14}$$

Here $G(x,s,k)$ is the Green's function of the operator $L = \frac{-d^2}{dx^2} + k^2$. Which means that $LG(x,s,k) = \delta(s-x)$.

The corresponding Green's function is the following:

$$G(x,s,k) = \begin{cases} -\frac{\sin k(x-s)}{k}, & x > s \\ 0, & x < s \end{cases}. \tag{A.15}$$

(Notice that when you differentiate $G(x,s,k)$ you get 0 for $x < s$ and $-\cos k(x-s)$ for $x > s$. so there is a jump from 0 to one at $x = s$. Therefore, the second derivative of G is given by: $-\delta(x-s) + k\sin k(x-s)$)

We can define the functions $\chi_+(x,k) = \phi(x,k)e^{ikx}$ and $\chi_-(x,k) = \psi(x,k)e^{ikx}$. Combining this with equations (A.14) and (A.15) gives:

$$\begin{aligned} \chi_+(x,k) &= 1 + \int_{-\infty}^{x} \frac{e^{2ik(x-s)} - 1}{2ik} u(s,k)\chi_+(s,k)ds \\ \chi_-(x,k) &= 1 - \int_{x}^{\infty} \frac{e^{2ik(x-s)} - 1}{2ik} u(s,k)\chi_-(s,k)ds. \end{aligned} \tag{A.16}$$

When $x \to -\infty$, χ_+ goes to 1, and u goes to zero rapidly enough, by assumption, to ensure convergence of the integral. So when $\Im(k) > 0$ the first integral in (A.16) is bounded. Therefore $\chi_+(x,k)$ and thus $\phi(x,k)$ is analytic in the upper half plane of k, and behaves asymptotically as: $\phi \to e^{-ikx}$, when $|k| \to \infty$ such that $\Im(k) > 0$. Similarly

$\psi(x,k)$ is analytic in the lower half plane of k with asymptotic behaviour: $\psi \to e^{ikx}$, when $|k| \to \infty$ such that $\Im(k) < 0$.

Earlier we stated that $a(k)$ was given by:

$$a(k) = \frac{1}{2ik} W(\phi(x,k), \overline{\psi}(x,\overline{k})). \tag{A.17}$$

Since, as shown above, $\psi(x,\overline{k})$ and $\phi(x,k)$ are both analytic in the upper-half k plane, $a(k)$ is analytic in the upper half k plane as well. Furthermore, $a(k_0) = 0$ implies $W(\phi(x,k_0), \overline{\psi}(x,\overline{k_0})) = 0$, and thus $\frac{\phi_x}{\phi} = \frac{\overline{\psi}(x,\overline{k_0})_x}{\overline{\psi}(x,\overline{k_0})}$. Integrating this gives:

$$\phi(x,k_0) = c'\overline{\psi}(x,\overline{k_0}). \tag{A.18}$$

This implies that $\phi(x,k_0)$ decreases exponentially as both $x \to \infty$ and $x \to -\infty$. Therefore $\phi(x,k_0)$ is a bound state eigenfunction, and thus k_0 is an eigenstate.

The zeros of a(k) are all simple. This can be shown in the following way. Firstly, differentiate equation (A.4) to obtain:

$$\partial_{xx}\partial_k\psi = (u - k^2)\partial_k\psi + 2k\psi. \tag{A.19}$$

If we take the derivative of $W(\partial_k\phi, \phi)$ with respect to x we get:

$$\partial_x W(\partial_k\phi, \phi) = \partial_k\phi\partial_{xx}\phi - \phi\partial_{xx}\partial_k\phi. \tag{A.20}$$

Using equations (A.19) and (A.4), we then find:

$$\partial_x W(\partial_k\phi, \phi) = \partial_k\phi(u - k^2)\phi - \phi(u - k^2)\partial_k\phi + 2k\phi^2 = 2k\phi^2. \tag{A.21}$$

Integrating both sides and using $\phi = 0$ for $x \to -\infty$ then gives the following result:

$$\lim_{x\to\infty} W(\partial_k\phi, \phi) = 2k \int_{-\infty}^{\infty} \phi^2 dx. \tag{A.22}$$

We can use this to show that, for a bound state eigenvalue $i\kappa_n$, $\partial_k a(i\kappa_n) \neq 0$. To do so, use: $a(k) = \frac{1}{2ik} W(\phi(x,k), \overline{\psi}(x,\overline{k}))$ and differentiate both sides w.r.t. k.

$$\begin{aligned} 2ik\partial_k a(k) &= \partial_k W(\phi(x,k), \overline{\psi}(x,\overline{k})) \\ &= W(\partial_k\phi(x,k), \overline{\psi}(x,\overline{k})) + W(\phi(x,k), \partial_k\overline{\psi}(x,\overline{k})) \\ &= \frac{1}{c_j} W((\partial_k\phi(x,k), \phi(x,k)) + c_j W(\overline{\psi}(x,\overline{k}), \partial_k\overline{\psi}(x,\overline{k})). \end{aligned}$$

In the limit $x \to \infty$ $W(\overline{\psi}(x,\overline{k}), \partial_k\overline{\psi}(x,\overline{k}))$ goes to zero. Therefore, taking this limit, and using the fact that $a(k)$ is independent of x gives:

$$ic_j \frac{da(i\kappa)}{dk} = \int_{-\infty}^{\infty} \phi^2 dx. \tag{A.23}$$

Since this integral is not equal to zero, the zeros of $a(k)$ are simple. Moreover, this shows the correspondence between the scattering data of the continuous spectrum, $a(k)$, and of the data of the discrete spectrum, c_j, through:

$$\frac{1}{\partial_k a(i\kappa_n)} = i\frac{c_n}{c'_n}. \tag{A.24}$$

The Fourier transform of $\chi_-(x,k) - 1$ w.r.t. k is given by:

$$A(x,s) = \int_{-\infty}^{\infty} e^{-iks}(\chi_- - 1)dk. \tag{A.25}$$

Since $\chi_-(x,k)-1$ is analytic in the upper-half plane and the integrand goes to zero in the limit $|k| \to \infty$ with $\Im(k) > 0$, when $s < 0$, contour integration tells us that $A(x,s) = 0$ when $y < 0$. Therefore we can write χ_- as:

$$\chi_-(x,k) = 1 + \frac{1}{2\pi}\int_0^{\infty} A(x,y)e^{iks}ds. \tag{A.26}$$

If we introduce $K(x,s) = \frac{1}{2\pi}A(x,s-x)$, then we can write the wavefunctions ψ_+ and ψ_- in the following way:

$$\begin{aligned} \psi_+(x,k) &= e^{ikx} + \int_x^{\infty} e^{iks}K(x,s)ds \\ \psi_-(x,k) &= e^{-ikx} + \int_x^{\infty} e^{-iks}K(x,s)ds. \end{aligned} \tag{A.27}$$

Now we are ready to prove that we can recover the potential from the scattering data by solving the Gelfand-Levitan-Marchenko-equation. We start by stating: $t(k)\phi_+ = \psi_- + r(k)\psi_+$. Combining this with the expressions for $\psi_\pm$ given by equation (A.27) we get:

$$t(k)\phi - e^{-ikx} = \int_x^{\infty} e^{-iks}K(x,s)ds + r(k)e^{ikx} + r(k)\int_x^{\infty} e^{iks}K(x,s)ds. \tag{A.28}$$

Now take the inverse Fourier transform, and write:

$$f_1(y) = \frac{1}{2\pi}\int_{-\infty}^{\infty} r(k)e^{iky}dk.$$

Then the inverse Fourier transform of the terms given in A.28 are:

$$\begin{aligned}
\frac{1}{2\pi}\int_{\infty}^{\infty} e^{iky}\int_{x}^{\infty} e^{-iks}K(x,s)dsdk &= K(x,y)\\
\frac{1}{2\pi}\int_{-\infty}^{\infty} e^{iky}e^{ikx}r(k)dk &= f_1(x+y)\\
\frac{1}{2\pi}\int_{-\infty}^{\infty} e^{iky}r(k)\int_{x}^{\infty} e^{iks}K(x,s)dsdk &= \int_{x}^{\infty} K(x,s)\frac{1}{2\pi}\int_{-\infty}^{\infty} e^{ik(y+s)}r(k)dkds\\
&= \int_{x}^{\infty} K(x,s)f_1(y+s)ds.
\end{aligned} \tag{A.29}$$

Now we also need to determine the inverse Fourier transform of the left-hand side of (A.28)

$$\frac{1}{2\pi}\int_{-\infty}^{\infty} e^{iky}[t(k)\phi(x,k)-e^{-ikx}]dk = \frac{1}{2\pi}\int_{-\infty}^{\infty} e^{ik(y-x)}[t(k)\phi(x,k)e^{ikx}-1]dk.$$

When $s > x$ this integral goes to zero for $|k| \to \infty$, $\Im(k) > 0$. Furthermore, the transmission coefficient; $t(k) = 1/a(k)$, has simple poles at the bound states $i\kappa_n$, with residue: $res(t(i\kappa_j)) = \frac{1}{\partial_k a(i\kappa_j)} = \frac{c_j}{c_j'}$. So contour integration over the upper half k plane gives:

$$i\sum_{j=1}^{N} res(t(i\kappa_j))e^{-\kappa_j y}\phi(x,i\kappa_j) \tag{A.30}$$

$$= i\sum_{j=1}^{N} c_j' res(t(i\kappa_j))e^{-\kappa_j y}\psi(x,i\kappa_j) \tag{A.31}$$

$$= i\sum_{j=1}^{N} c_j\big[e^{-\kappa_j(x+y)} + \int_{x}^{\infty} e^{-\kappa_j(s+y)}K(x,s)ds\big] \tag{A.32}$$

$$= -f_2(x+y) - \int_{x}^{\infty} f_2(s+y)K(x,s)ds. \tag{A.33}$$

Where $f_2(x) = -i\sum_{j=1}^{N} c_j e^{-\kappa_j x}$.

Putting all these terms into equation (A.28) we get:

$$-f_2(x+y) - \int_{x}^{\infty} f_2(s+y)K(x,s)ds = K(x,y) + f_1(x+y) + \int_{x}^{\infty} K(x,s)f_1(y+s)ds. \tag{A.34}$$

Writing $B(x) = f_1 + f_2$ we then obtain the Gelfand-Levitan-Marchenko equation(A.1):

$$K(x,s) + B(x+s) + \int_{x}^{\infty} B(s+z)K(x,z)dz = 0. \tag{A.35}$$

The only thing left to show is $u(x) = -\frac{d}{dx}K(x,x)$. To do this we take $\frac{d^2}{dx^2}\psi + (k^2 - u)\psi = 0$ and use (A.27). We get:

$$0 \;=\; -e^{ikx}u(x) \;+\; \int_x^\infty e^{iks}(k^2 \;-\; u(x))K(x,s)ds \;+\; \frac{d^2}{dx^2}\int_x^\infty e^{iks}K(x,s)ds \quad \text{(A.36)}$$

We can use the following to express the rightmost term:

$$\begin{aligned}\frac{d^2}{dx^2}\int_x^\infty g(x,s)ds &= \frac{d^2}{dx^2}(-G(x,x) + \lim_{y\to\infty} G(x,y)) \\ &= -\frac{d}{dx}(g(x,x) + G_x(x,x)) + \lim_{y\to\infty} G_{xx}(x,y) \\ &= -\frac{d}{dx}g(x,x) - g_x(x,x) - G_{xx}(x,x) + \lim_{y\to\infty} G_{xx}(x,y) \\ &= -\frac{d}{dx}g(x,x) - g_x(x,x) + \int_x^\infty \frac{d^2}{dx^2}g(x,s)ds,\end{aligned}$$

where $G(x,s)$ is the integrand of $g(x,s)$ w.r.t. s, and $g_x(x,x)$ means evaluating the x-derivative of g at (x,x), to write (A.36) as:

$$0 = -e^{ikx}u(x) + \int_x^\infty e^{iks}(k^2 - u(x) + \frac{d^2}{dx^2})K(x,s)ds - e^{iks}(K_x(x,x) + \frac{d}{dx}K(x,x) + ikK(x,x)) \quad \text{(A.37)}$$

If we then use the fact that $k^2e^{iks} = -\frac{d^2}{ds^2}e^{iks}$, and partial integration we get:

$$\begin{aligned}\int_x^\infty e^{iks}k^2K(x,s)ds &= -\int_x^\infty \frac{d^2e^{iks}}{ds^2}K(x,s)ds \\ &= -ikK(x,x)e^{ikx} + K_s(x,x)e^{ikx} - \int_x^\infty K_{ss}(x,s)e^{iks}ds\end{aligned}$$

And thus:

$$\int_x^\infty (K_{xx} + K_{ss} + uK)(x,s)e^{ik(s-x)}ds - (2\frac{d}{dx}K(x,x) + u(x)) = 0 \quad \text{(A.38)}$$

If we let $\Im(k) \to +\infty$. The integral on the left side of (A.38) goes to zero, because $s > x$. Therefore $2\frac{d}{dx}K(x,x) = -u(x)$, since this term does not depend on k, it should hold for all k therefore:

$$2\frac{d}{dx}K(x,x) = -u(x) \quad \text{(A.39)}$$

B Figures

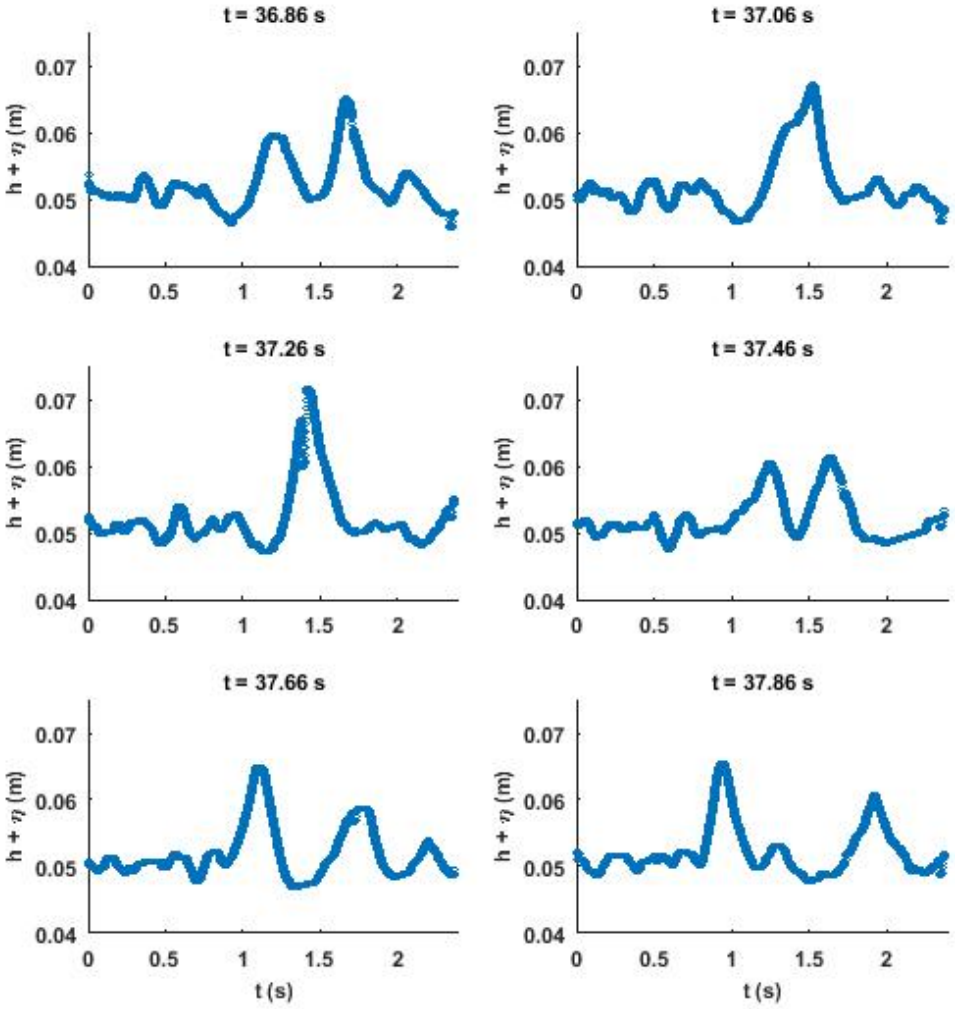

Figure B.1: Collision 1

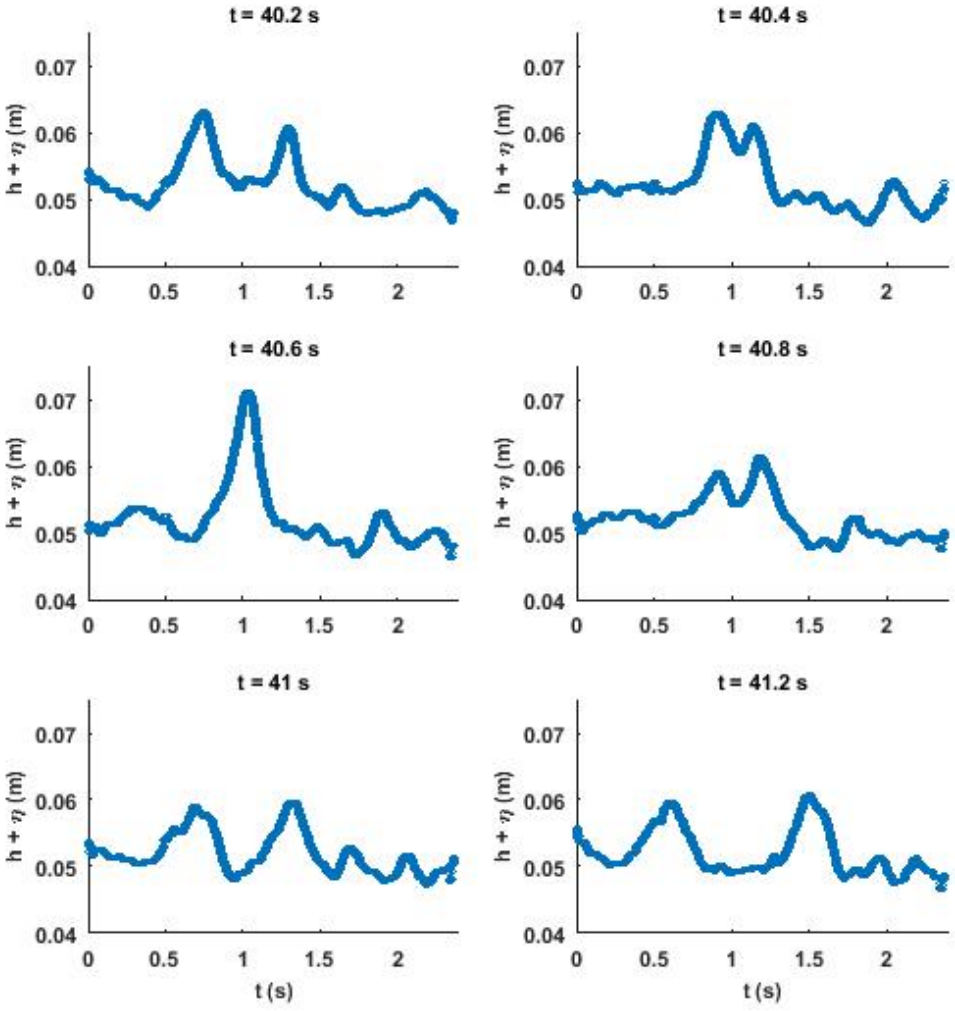

Figure B.2: Collision 2

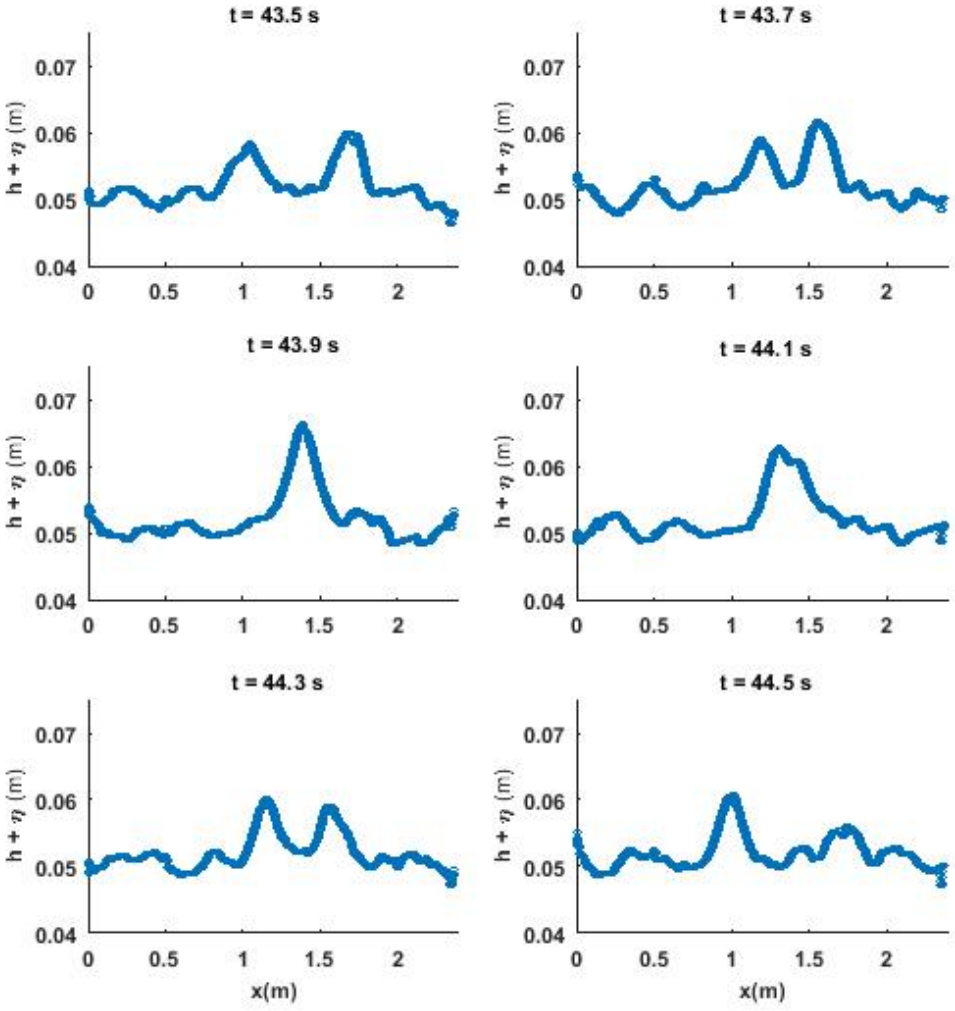

Figure B.3: Collision 3

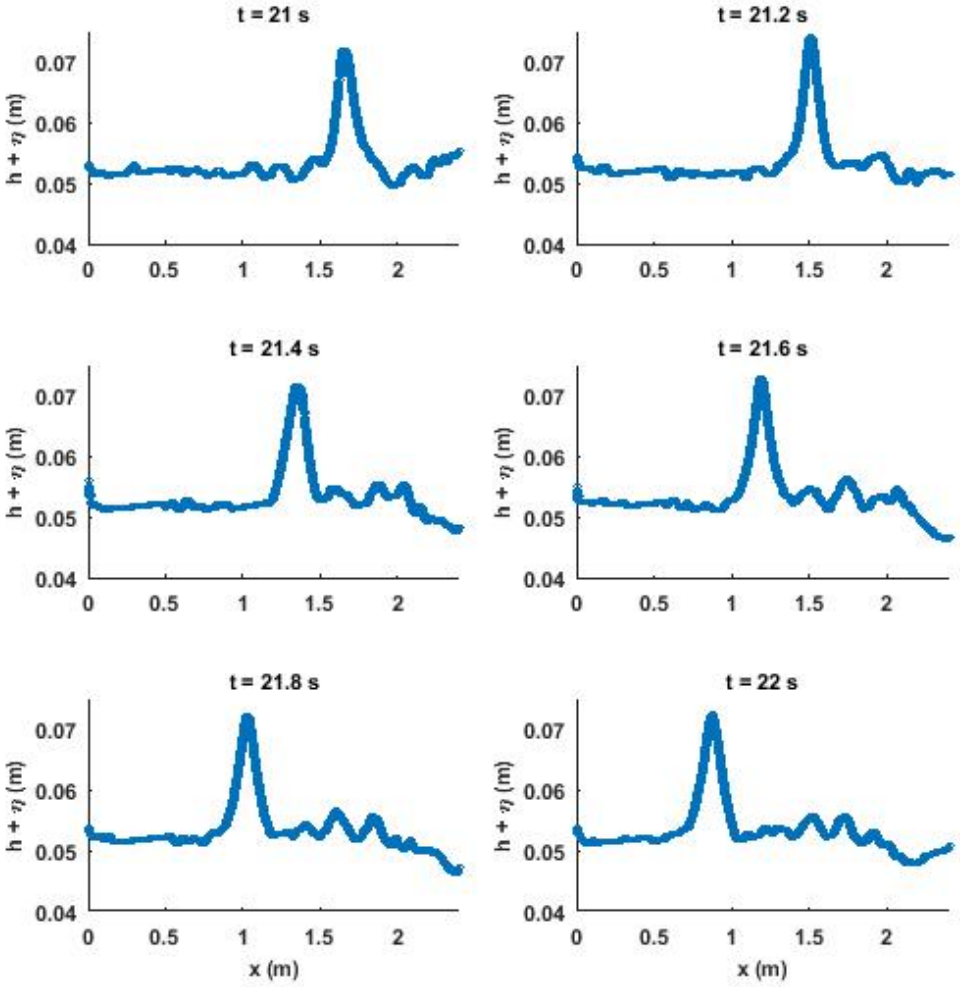

Figure B.4: Soliton between the first and second reflection.

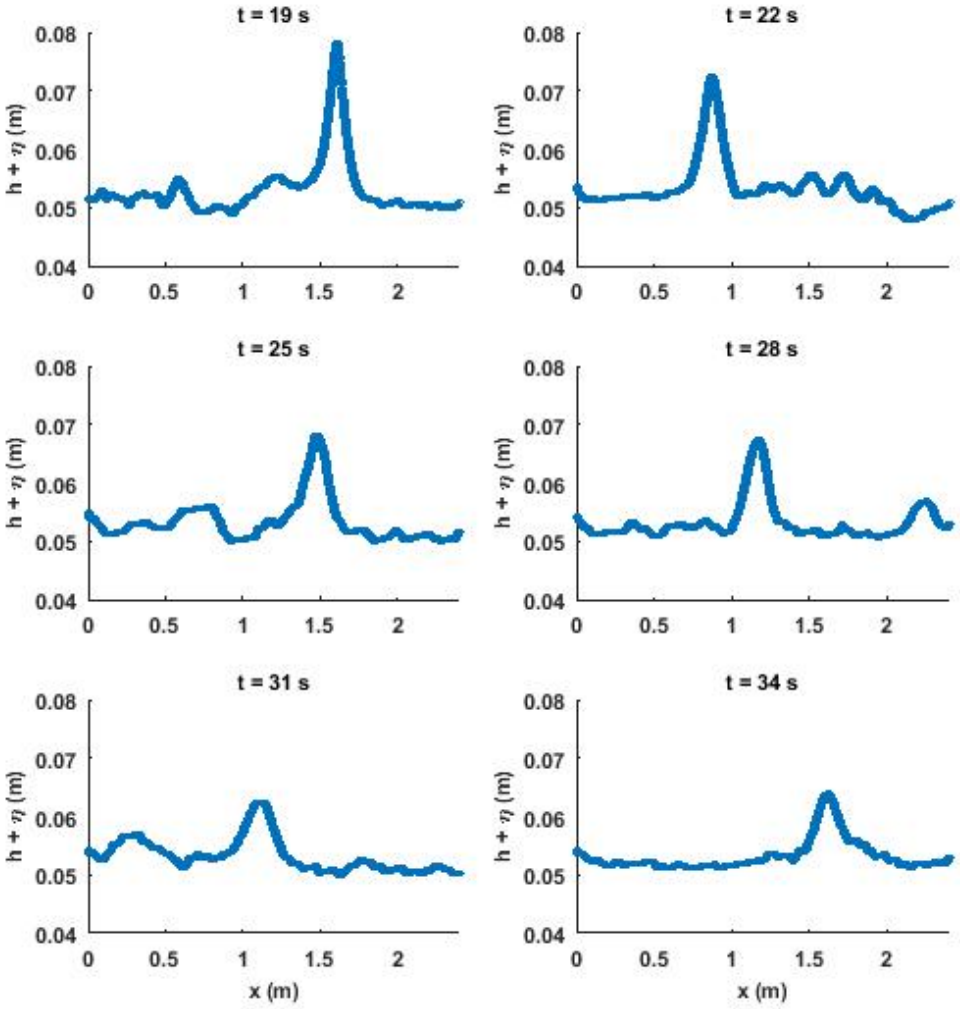

Figure B.5: Decrease of amplitude of a single soliton after reflections.

References

[1] G. B Whitham. *Linear and Non-linear Waves.* Wiley, New York, 1974.

[2] M. Tabor. *Chaos and integrability in nonlinear dynamics: an introduction.* Wiley, New York, 1989.

[3] W. Craig, P. Guyenne, J. Hammack, D. Henderson, and C. Sulem. Solitary water wave interactions. *Physics of Fluids*, 18(5):1–25, 2006.

[4] T Maxworthy. Experiments on collisions between solitary waves. *Journal of Fluid Mechanics*, 76(01):177–186, 1976.

[5] M. J. Cooker, P. D. Weidman, and D. S. Bale. Reflection of a high-amplitude solitary wave at a vertical wall. *Journal of Fluid Mechanics*, 342(1):141–158, 1997.

[6] H. Power and Allen T. Chwang. On reflections of a planer solitary wave at a vertical wall. *Wave Motion*, 6(2):183–195, 1984.

[7] S. Novikov, S.V. Manakov, L.P. Pitaevskii, and V.E. Zakharov. *Theory of Solitons: The Inverse Scattering Method.* Monographs in Contemporary Mathematics. Springer US, 1984.

[8] D.H. Sattinger. Scaling, mathematical modelling, and integrable systems, 1998.